

Radiative charge-transfer lifetime of the excited state of $(\text{NaCa})^+$

Oleg P. Makarov,* R. Côté, H. Michels, and W. W. Smith

Department of Physics, University of Connecticut, Storrs, Connecticut 06269-3046

(Received 17 September 2002; revised manuscript received 23 January 2003; published 11 April 2003)

New experiments were proposed recently to investigate the regime of cold atomic and molecular ion-atom collision processes in a special hybrid neutral-atom-ion trap under high-vacuum conditions. We study the collisional cooling of laser precooled Ca^+ ions by ultracold Na atoms. Modeling this process requires knowledge of the radiative lifetime of the excited singlet $A^1\Sigma^+$ state of the $(\text{NaCa})^+$ molecular system. We calculate the rate coefficient for radiative charge transfer using a semiclassical approach. The dipole radial matrix elements between the ground and the excited states, and the potential curves were calculated using complete active space self-consistent field and Möller-Plesset second-order perturbation theory with an extended Gaussian basis, 6-311+G (3df). The semiclassical charge-transfer rate coefficient was averaged over a thermal Maxwellian distribution. In addition, we also present elastic collision cross sections and the spin-exchange cross section. The rate coefficient for charge transfer was found to be 2.3×10^{-16} cm^3/sec , while those for the elastic and spin-exchange cross sections were found to be several orders of magnitude higher (1.1×10^{-8} cm^3/sec and 2.3×10^{-9} cm^3/sec , respectively). This confirms our assumption that the milli-Kelvin regime of collisional cooling of calcium ions by sodium atoms is favorable with the respect to low loss of calcium ions due to the charge transfer.

DOI: 10.1103/PhysRevA.67.042705

PACS number(s): 32.80.Pj, 34.80.Qb, 82.20.Pm, 82.30.Fi

I. INTRODUCTION

A broad range of techniques from atomic physics and optics have allowed the accurate manipulation of ultracold samples. Recent studies are probing ultracold atomic systems in which electric charges may play an important role [1–3]. These include ultracold plasmas [4–7], ultracold Rydberg gases [8,9], as well as ionization experiments in a Bose-Einstein condensate [10].

Recently, we proposed experiments on simultaneously cooling and trapping ions and atoms in the same confined space [11]. The proposed experiments will investigate the regime of cold atomic and molecular ion-atom collision processes in a special hybrid neutral-atom-ion trap under high-vacuum collisions. The idea is to use the techniques of laser cooling, trapping, and manipulation of cold neutral atoms to make a refrigerator for the sympathetic cooling of an overlapping sample of atomic or molecular ions to very low temperatures. We intend to probe fundamental collision processes and cooling kinetics in as low a temperature range as possible.

The hybrid trap we have built consists of a conventional magneto-optic neutral-atom trap (MOT) combined with a linear Paul radio frequency quadrupole trap. The linear Paul trap, with longitudinal electrostatic confinement, is chosen so as to suppress most of the micromotion and rf heating associated with conventional Paul traps [12].

II. POTENTIAL CURVES AND DIPOLE MOMENT

To calculate the cross sections and rate coefficients for the charge transfer and the elastic and spin-exchange collisions, we have performed *ab initio* calculations of the adiabatic

potential curves for the $(\text{NaCa})^+$ molecular system in the $X^1\Sigma^+$, $a^3\Sigma^+$, and $A^1\Sigma^+$ states, which go asymptotically to the ground $(\text{Na}^+ + \text{Ca})$ and excited $[\text{Ca}^+ + \text{Na}(3s)]$ states of the ion-atom quasimolecular system. The method used was second-order Möller-Plesset perturbation theory (MP2) using a Gaussian triple ζ +diffuse+polarization basis set, 6-311+G (3df). This basis set included three sets of *d*-polarization functions and one set of *f*-polarization functions in addition to a diffuse function on each atomic center. The first excited $A^1\Sigma^+$ state was optimized for the second root of a CASSCF (complete active space self-consistent field) using eight orbitals in the active space. This was followed with an MP2 correction to the optimized CASSCF energy.

Figure 1 shows the potential curves of the ground and excited states of $(\text{NaCa})^+$ molecular system in atomic units

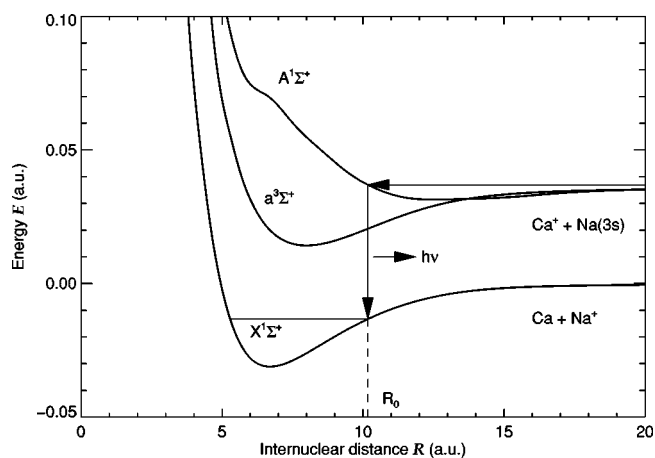


FIG. 1. Adiabatic potential curves for selected states of the $(\text{NaCa})^+$ molecular system. R_0 is a classical turning point. Shown is a free-bound radiative transition with the emission of a photon $h\nu$.

*Electronic address: Oleg.Makarov@UConn.edu

TABLE I. Potential energy and dipole matrix element values obtained by cubic spline fit of the adiabatic potential and dipole matrix curves for selected states of the $(\text{NaCa})^+$ molecular system. Potential curves are located relative to the ground asymptote. Notation $1.23[-4]$ stands for 1.23×10^{-4} .

R (a_0)	$X^1\Sigma^+$	E (a.u.)		d (a.u.)
		$A^1\Sigma^+$	$a^3\Sigma^+$	
3	3.54[-1]	4.16[-1]	1.25	
4	7.42[-2]	1.98[-1]	2.28[-1]	
5	-2.15[-3]	1.09[-1]	6.88[-2]	
6	-2.79[-2]	7.47[-2]	3.15[-2]	
7	-3.07[-2]	6.64[-2]	1.73[-2]	8.80[-1]
8	-2.61[-2]	5.47[-2]	1.42[-2]	8.47[-1]
9	-1.99[-2]	4.55[-2]	1.60[-2]	7.49[-1]
10	-1.42[-2]	3.79[-2]	1.98[-2]	6.08[-1]
11	-9.64[-3]	3.34[-2]	2.39[-2]	4.63[-1]
12	-6.30[-3]	3.16[-2]	2.75[-2]	3.32[-1]
13	-4.01[-3]	3.15[-2]	3.03[-2]	2.22[-1]
14	-2.56[-3]	3.18[-2]	3.22[-2]	1.38[-1]
15	-1.70[-3]	3.22[-2]	3.33[-2]	7.90[-2]
16	-1.21[-3]	3.30[-2]	3.41[-2]	4.15[-2]
17	-9.17[-4]	3.39[-2]	3.45[-2]	2.04[-2]
18	-7.24[-4]	3.45[-2]	3.48[-2]	9.44[-3]
19	-5.84[-4]	3.49[-2]	3.51[-2]	4.21[-3]
20	-4.76[-4]	3.52[-2]	3.52[-2]	1.53[-3]

(see also Table I). The curves were obtained by performing a cubic spline fit to the calculated points. At small internuclear separations R , the potential curves were approximated with the short-range potential of the form $V(R) = (A/R)\exp(-BR)$, where A and B are fitting parameters, and for $R > 30a_0$, the potential curves were fitted with the appropriate long-range potentials. For the excited states, the long-range potential was of the form

$$V(R) \sim -\frac{1}{2} \left(\frac{162.7}{R^4} + \frac{1902}{R^6} + \frac{55518}{R^8} \right), \quad (1)$$

where the Na dipole (162.7 a.u.), quadrupole (1902 a.u.), and octupole (55,518 a.u.) polarizabilities were taken from Ref. [1]. For the ground state $X^1\Sigma^+$, the form of the long-range potential was

$$V(R) \sim -\frac{1}{2} \frac{\alpha_d}{R^4}, \quad (2)$$

where $\alpha_d = 156$ a.u. is the dipole polarizability of the calcium atom.

Figure 2 shows the calculated radial dipole matrix element between $X^1\Sigma^+$ and $A^1\Sigma^+$ states fitted with cubic splines (see also Table I). The dipole matrix elements were calculated for $R > 8a_0$ only, since for our purposes the problem did not require the exact knowledge of the dipole radial matrix elements at smaller distances. At small distances there

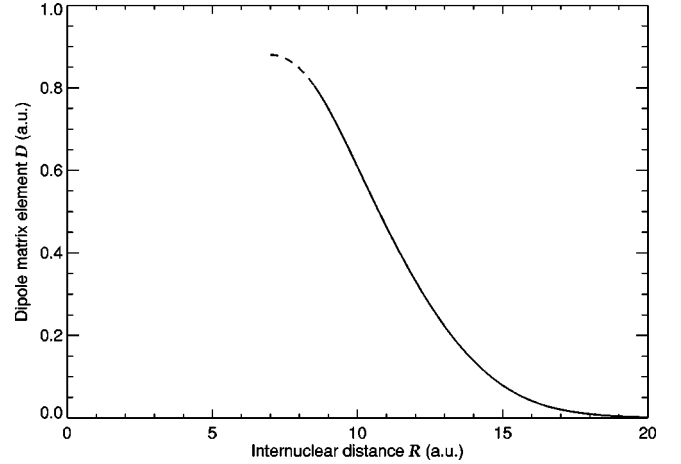


FIG. 2. Calculated radial transition dipole matrix elements. The matrix elements are calculated at distances $R > 8a_0$ only, because the current problem does not require the knowledge of the matrix elements at lower internuclear distances due to small energies of the approaching sodium atoms.

is little overlap between the wave functions of the ground and excited states for the energies of the approaching sodium atoms considered here. At milli-Kelvin energies of the sodium atoms, the classical turning point R_0 was found to be always to the right of $R = 8a_0$.

III. CROSS SECTIONS

A neutral atom of Na collides elastically with Ca^+ in the singlet $A^1\Sigma^+$ or triplet $a^3\Sigma^+$ states of NaCa^+ . The corresponding elastic cross sections are given by

$$\sigma_{\text{el}}^{S,T} = \frac{4\pi}{k^2} \sum_{l=0}^{\infty} (2l+1) \sin^2(\eta_l^{S,T}), \quad (3)$$

where $k = \sqrt{2\mu E}/\hbar$ with μ the reduced mass and E the collision energy in the center of mass of the system, and $\eta_l^{S,T}$ is the l th partial-wave phase shift corresponding to the $A^1\Sigma^+$ and $a^3\Sigma^+$ states, respectively. Another possible outcome of the collision between Na and Ca^+ is spin exchange. In the elastic approximation [13], also known as the degenerate internal states approximation [14], one describes this scattering process in terms of the singlet- and triplet-scattering phase shifts, and the spin-exchange cross section is given by

$$\sigma_{\text{exch.}} = \frac{\pi}{k^2} \sum_{l=0}^{\infty} (2l+1) \sin^2(\eta_l^S - \eta_l^T). \quad (4)$$

Although this approximation is valid for collision energies larger than the hyperfine splitting, it usually gives the right order of magnitude at smaller energies [15].

The phase shifts $\eta_l^{S,T}$ are determined from the continuum eigenfunctions $y_{E,l}^{S,T}(R)$, which are the regular solutions of the partial-wave equation

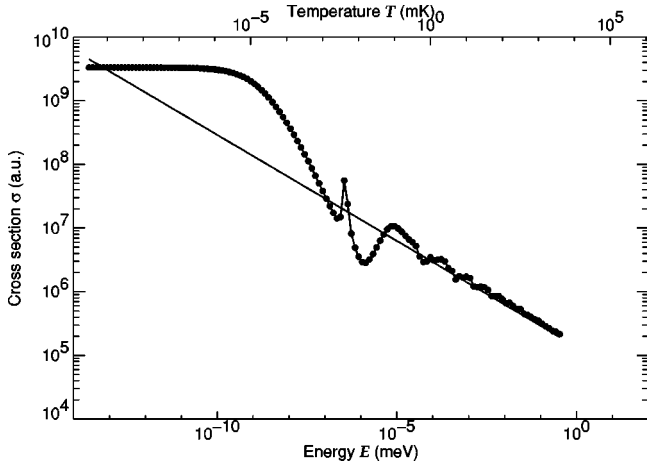


FIG. 3. Elastic collision cross section for the $A^1\Sigma^+$ state of molecular system $(\text{NaCa})^+$. The elastic cross section above $10 \mu\text{K}$ fits the approximate expression $\sigma(E) = 5310E^{-1/3}$, where the energy is in units of Hartrees and the cross section is in units of a_0^2 .

$$\left(\frac{d^2}{dR^2} + k^2 - \frac{2\mu}{\hbar^2} V_{s,T}(R) - \frac{l(l+1)}{R^2} \right) y_{E,l}^{S,T}(R) = 0. \quad (5)$$

The asymptotic form of $y_{E,l}^{S,T}(R)$ at large distances gives the elastic scattering phase shifts

$$y_{E,l}^{S,T}(R) \sim \sin \left[kR - \frac{l\pi}{2} + \eta_l^{S,T}(k) \right]. \quad (6)$$

The results of our calculations are shown on Figs. 3 and 4 for the singlet and triplet elastic cross sections, respectively, and on Fig. 5 for the spin-exchange cross section. In all cases, the s -wave contribution is dominant at energies corresponding to temperatures below 1 nK , in sharp contrast to neutral alkali atoms where this takes place for energies around $100 \mu\text{K}$ [16]. This is due to the very long range of the polarization potential as compared to the shorter range of

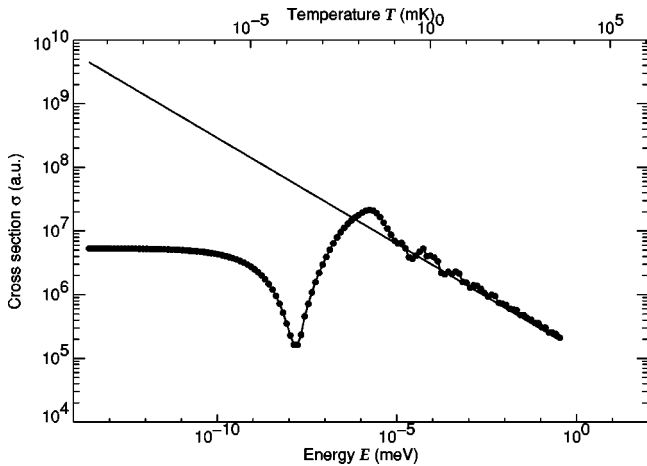


FIG. 4. Elastic collision cross section for the $a^3\Sigma^+$ state of molecular system $(\text{NaCa})^+$. The elastic cross section above $10 \mu\text{K}$ fits the approximate expression $\sigma(E) = 5070E^{-1/3}$, where the energy is in units of Hartrees and the cross section is in units of a_0^2 .

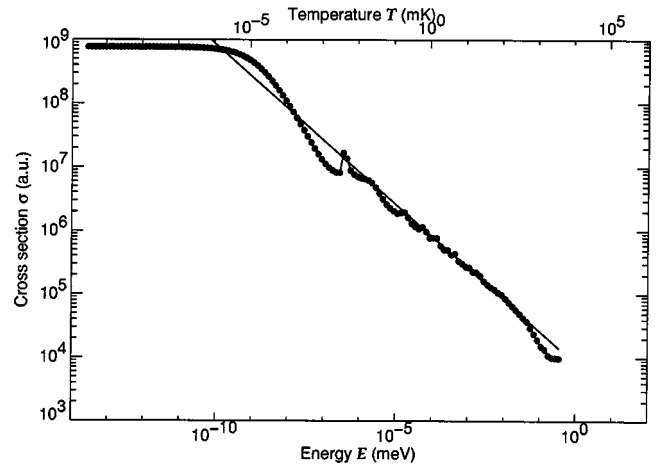


FIG. 5. Spin-exchange collision cross section between states $A^1\Sigma^+$ and $a^3\Sigma^+$ of the molecular system $(\text{NaCa})^+$. The cross section fits the expression $\sigma(E) = 44E^{-1/2}$, where the energy is in units of Hartrees and the cross section is in units of a_0^2 .

van der Waals interactions between neutral atoms. Our *ab initio* potential curves are not of sufficient accuracy to predict the s -wave scattering lengths associated with the singlet and triplet potentials with a high degree of certainty: the measurements that will be realized in our proposed hybrid MOT would help fine-tuning the potentials so that accurate estimates of the scattering lengths could be given. As E increases, many more partial waves contribute to the cross sections: already at $E/k_B \sim 1 \mu\text{K}$, seven partial waves are necessary, and over 30 are required at 1 mK . Although shape resonances may play an important role at very small energies, their effect is not dominant for E/k_B larger than $100 \mu\text{K}$ (see the smooth behavior of the cross sections in Figs. 3–5). This rapid growth in the number of partial waves led us to consider semiclassical approximations for the cross sections. Following the method described in Ref. [1], we found that the cross sections are well represented by power-law functions of energy for the temperature range down to μK . Figures 3–5 show the calculated collision cross sections together with the power-law fits

$$\sigma_{\text{el.}}(E) = C_{\text{el.}} E^{-1/3}, \quad (7)$$

$$\sigma_{\text{exch.}}(E) = C_{\text{exch.}} E^{-1/2}, \quad (8)$$

where $C_{\text{el.}} = 5310$ and 5070 for the singlet $A^1\Sigma^+$ and triplet $a^3\Sigma^+$ states, respectively, and $C_{\text{exch.}} = 44$. These coefficients were obtained by performing a linear fit of the cross sections plotted on a log-log scale in the energy range above $1 \mu\text{K}$, all quantities expressed in atomic units.

Using these approximate cross sections, we can calculate the various rate coefficients $\mathcal{R} = \langle \sigma v \rangle$, where $v = \sqrt{2E/\mu}$ is the relative velocity, and $\langle \dots \rangle$ implies averaging over the velocity distribution. Assuming a Maxwellian velocity distribution characterized by the temperature T , we obtain the following rate coefficients:

$$\mathcal{R}_{\text{el.}} = \sqrt{\frac{8}{\pi\mu}} \Gamma\left(\frac{5}{3}\right) (k_B T)^{1/6} C_{\text{el.}}, \quad (9)$$

$$\mathcal{R}_{\text{exch.}} = \sqrt{\frac{2}{\mu}} C_{\text{exch.}}, \quad (10)$$

in atomic units. Note that while $\mathcal{R}_{\text{exch.}}$ is independent of temperature, $\mathcal{R}_{\text{el.}}$ varies very slowly with T . Figures 3–5 show that the power-law fits are valid at temperatures 1–10 μK and higher, which validates the semiclassical approach to calculating the rate coefficients for elastic and spin-exchange collisions.

As an example, suitable for the proposed experiment, we evaluated the rates for a temperature of 1 mK. They are $\mathcal{R}_{\text{el.}} = 1.7\text{--}1.8$ a.u. for elastic collisions and $\mathcal{R}_{\text{exch.}} = 0.38$ a.u. for spin-exchange collisions. Converting to units $\text{cm}^3 \text{sec}^{-1}$, we obtain $\mathcal{R}_{\text{el.}} = (1.05\text{--}1.10) \times 10^{-8} \text{cm}^3 \text{sec}^{-1}$ and $\mathcal{R}_{\text{exch.}} = 2.33 \times 10^{-9} \text{cm}^3 \text{sec}^{-1}$. For a typical MOT particle density $n = 10^{10} \text{cm}^{-3}$ these rates give the following values for effective elastic lifetimes $1/\tau: 1/\tau_{\text{el.}} = \mathcal{R}_{\text{el.}} n = (1.05\text{--}1.10) \times 10^2 \text{sec}^{-1}$ and $1/\tau_{\text{exch.}} = \mathcal{R}_{\text{exch.}} n = 23.3 \text{sec}^{-1}$.

IV. RADIATIVE CHARGE TRANSFER

The rate coefficient for radiative charge transfer may be expressed as an integral of the transition probability over the collision path, averaged over the initial velocities and the impact parameters [17]. Because many partial waves contribute even at 1 μK , we use a semiclassical treatment where the cross section for radiative charge transfer may be expressed as [18]

$$\sigma_{\text{tr}} = 2\pi \left(\frac{2\mu}{E}\right)^{1/2} \int_0^\infty b db \int_{R_0}^\infty dR \frac{A(R)}{[1 - V(R)/E - b^2/R^2]^{1/2}}, \quad (11)$$

where b is the impact parameter, R_0 is the classical turning point (distance of closest approach), $A(R)$ is the Einstein spontaneous emission transition probability, and $V(R)$ is the entrance channel potential curve. Again, we can obtain a rate coefficient $\mathcal{R}_{\text{tr}} = \langle \sigma v \rangle$ by averaging over a Maxwellian velocity distribution characterized by T [19],

$$\mathcal{R}_{\text{tr}} = 8\sqrt{\pi} \left(\frac{1}{k_B T}\right)^{3/2} \int_0^\infty dE \int_0^\infty db \times \int_{R_0}^\infty dR \frac{b E^{1/2} A(R) e^{-E/k_B T}}{[1 - b^2/R^2 - V(R)/E]^{1/2}}. \quad (12)$$

The transition probabilities are approximated by

$$A(R) = \frac{4}{3} \alpha^3 \omega^3(R) D(R) \text{ a.u.}, \quad (13)$$

where α is the fine-structure constant, $D(R)$ is the dipole moment (see Fig. 2), and

$$\hbar \omega(R) = V_n(R) - V_{n'}(R) \quad (14)$$

is the energy difference between the entrance and exit potential curves (here $A^1\Sigma^+$ and $X^1\Sigma^+$, respectively), all at a separation R . Note that the effect of possible shape resonances is not taken into account in Eq. (12): as mentioned in the preceding section, shape resonances are not relevant for $E/k_B \sim 100 \mu\text{K}$ or higher (although they may play a role at much lower energies). The integrations of the Eq. (12) were evaluated numerically for temperatures ranging from 1 mK to 1000 K. The rate coefficient was found to be practically constant with the value of $\mathcal{R}_{\text{tr}} = 2.3 \times 10^{-16} \text{cm}^3/\text{sec}$. With the attainable densities of ultracold sodium atoms of the order of $n = 10^9\text{--}10^{11} \text{cm}^{-3}$, the rate coefficient gives for the the radiative lifetime of the excited $A^1\Sigma^+$ state

$$\tau_{\text{tr}} = 1/(\mathcal{R}_{\text{tr}} n) \sim 4 \times 10^4\text{--}4 \times 10^6 \text{sec}, \quad (15)$$

or in the range from several hours to several days. Parenthetically, we note that, although charge transfer *without* photon emission is possible at higher collision energies (many eV), in the 1 K range and below, the small coupling between the a and X states of $(\text{NaCa})^+$ (see Fig. 1) makes the rate for nonradiative charge transfer negligible.

We also considered the possibility of a charge-transfer process that could occur by laser excitation from the $A^1\Sigma^+$ state of NaCa^+ to a higher molecular state that correlates with $\text{Na}^+(3s)$ plus an excited Ca level. The two wavelengths that must be considered are $\text{Na}(3s \rightarrow 3p)$ at 589.0 nm and $\text{Ca}^+(4s \rightarrow 4p)$ at 397.0 nm. An examination of the asymptotic limits of molecular states lying above $\text{Na}(3s) + \text{Ca}^+(4s)$ indicates that the closest excited level would correspond to $\text{Na}^+(3s) + \text{Ca}[^1P(4p)]$ at 633.0 nm, too far from resonance to be of importance [20].

V. CONCLUSION

In conclusion, we have shown that the semiclassical approach for evaluating the rate coefficients is a good approximation because many partial waves are involved even at ~ 1 mK. The excited singlet state of the colliding molecular system $(\text{NaCa})^+$ is metastable against radiative charge transfer with the lifetime of the order of many hours. At the same time, the rates for elastic collisions and also for spin exchange are much greater, which provides an efficient mechanism for sympathetic collisional cooling of calcium ions by sodium atoms in the meV regime and below. We are setting up an experiment to measure collisional cooling by this mechanism.

ACKNOWLEDGMENTS

This work is supported in part by NSF Grant Nos. PHY-9988215 (O.M. and W.S.) and PHY-0140290 (R.C.), as well as the University of Connecticut Research Foundation (R.C.) and the Research Corporation (R.C.).

- [1] R. Côté and A. Dalgarno, *Phys. Rev. A* **62**, 012709 (2000).
- [2] R. Côté, *Phys. Rev. Lett.* **85**, 5316 (2000).
- [3] R. Côté, V. Kharchenko, and M.D. Lukin, *Phys. Rev. Lett.* **89**, 093001 (2002), this paper was selected to be part of the August 19, 2002 issue of the *Virtual Journal of Nanoscale Science & Technology* (<http://www.vjnano.org>).
- [4] T.C. Killian, S. Kulin, S.D. Bergeson, L.A. Orozco, C. Orzel, and S.L. Rolston, *Phys. Rev. Lett.* **83**, 4776 (1999).
- [5] T.C. Killian, M.J. Lim, S. Kulin, R. Dumke, S.D. Bergeson, and S.L. Rolston, *Phys. Rev. Lett.* **86**, 3759 (2001).
- [6] S. Kulin, T.C. Killian, S.D. Bergeson, and S.L. Rolston, *Phys. Rev. Lett.* **85**, 318 (2000).
- [7] E. Eyler and P. L. Gould (private communication).
- [8] W.R. Anderson, J.R. Veale, and T.F. Gallagher, *Phys. Rev. Lett.* **80**, 249 (1998).
- [9] I. Mourachko, D. Comparat, F. de Tomasi, A. Fioretti, P. Nosbaum, V.M. Akulin, and P. Pillet, *Phys. Rev. Lett.* **80**, 253 (1998).
- [10] D. Ciampini, M. Anderlini, J.H. Müller, F. Fuso, O. Morsch, J.W. Thomsen, and E. Arimondo, e-print physics/0206019.
- [11] W.W. Smith, E. Babenko, R. Côté, and H.H. Michels, in *Proceedings of the Eighth Rochester Conference on Coherence and Quantum Optics*, edited by N. Bigelow (Plenum, New York, 2002).
- [12] M.G. Raizen, J.M. Gilligan, J.C. Bergquist, W.M. Itano, and D.J. Wineland, *Phys. Rev. A* **45**, 6493 (1992).
- [13] A. Dalgarno and M.R.H. Rudge, *Proc. R. Soc. London, Ser. A* **286**, 519 (1965).
- [14] B.J. Verhaar, J.M.V.A. Koelman, H.T.C. Stoof, O.J. Luiten, and S.B. Crampton, *Phys. Rev. A* **35**, 3825 (1987).
- [15] E. Timmermans and R. Côté, *Phys. Rev. Lett.* **80**, 3419 (1998).
- [16] J. Weiner, V.S. Bagnato, S.C. Zilio, and P.S. Julienne, *Rev. Mod. Phys.* **71**, 1 (1999).
- [17] D.R. Bates, *Mon. Not. R. Astron. Soc.* **111**, 303 (1951).
- [18] B. Zygelman and A. Dalgarno, *Phys. Rev. A* **38**, 1877 (1988).
- [19] S.E. Butler, S.L. Guberman, and A. Dalgarno, *Phys. Rev. A* **16**, 500 (1977).
- [20] A second stimulated emission process could possibly arise since the $\text{Na}^+ + \text{Ca}[^1S(5s)]$ asymptote is close (392.7 nm) to the Ca^+ resonance line at 397.0 nm. Excitation to this level, however, can be eliminated in the experiment by turning off the 397.0-nm ion cooling laser before activating the MOT.